Abstract

Thin sections of pleura and lung prepared for diagnosis of Malignant Mesothelioma (MM) in patients who underwent pleurodesis were analysed by micro-Raman spectroscopy. In the pleural tissue, visual inspection under an optical microscope attached to the Raman spectroscope revealed numerous acicular crystals and several rounded particles, micrometers in size. The laser beam of the spectrometer was focused on each of the inorganic phases in turn, revealing Raman spectra attributable to talc or to clinochlore on the acicular crystals and to phosphate phases on the rounded particles. In the lung tissue, optical inspection indicated the presence of asbestos bodies, identified by micro-Raman spectroscopy as crocidolite, “asbestos” mineral, the phase of the fibre inside the coating material. The identity of the inorganic phases as determined by Raman spectroscopy was confirmed by chemical analysis using a Scanning Electron Microscope equipped with an Energy Dispersive Spectrometer (SEM/EDS). Micro-Raman spectroscopy proved effective in identifying the inorganic phases present in thin sections prepared for medical diagnosis, allowing compounds introduced during treatment (talc or clinochlore) to be distinguished from those inhaled (asbestos) or crystallized during disease progression (phosphates).

1. Introduction

Malignant Mesothelioma (MM) is an aggressive form of pulmonary cancer strongly associated with asbestos exposure [1], [2], [3], [4], [5], [6], [7], [8], [9], [10], [11], [12], [13] and [14]. Its diagnosis can be suspected from analysis of pleural liquid or a fragment of neoplasia by trans-chest biopsy but can only be definitely confirmed by surgical specimen or post-mortem analysis. Identifying biological markers for asbestos exposure is thus of great interest in resolving the complex medico-legal problems, often associated with the disease. A number of biological markers are under investigation, including pleural plaques revealed by radiological tests and observations made by Optical Microscopy (OM) and/or Electron Microscopy (EM) of cytological/histological sections taken during surgical treatment of uncovered and/or covered asbestos fibres (“asbestos bodies”). In recent years, our research group has been using micro-Raman spectroscopy to identify the mineral phases in histological sections from patients affected by important respiratory diseases, without digestion of the organic matrix [15] and [16]. This technique could help the investigations, and we would confirm it as reliable also when mesothelioma is treated with talc injection during pleurodesis, a commonly used palliative procedure in MM for the prevention of recurrent fluid accumulation. Pleurodesis consists of the introduction of a sclerosing agent to achieve the symphysis of visceral and parietal pleura. Talc is recognized by the American Thoracic Society and European Respiratory Society Task Force for the management of malignant pleural effusion as the best sclerosing agent, although talc itself can be involved in pulmonary diseases. In fact, pleural tissue responds to talc by developing a foreign body granuloma, often appearing as foreign body giant cells, containing crystalline materials. The term talco-silicosis or talco-asbestosis is sometimes applied to the resulting pneumoconiosis, especially when the talc is contaminated by silica or by asbestos phases. Deposits of ferruginous bodies, very similar to those induced by asbestos, have also

been described [17], [18], [19], [20], [21], [22], [23] and [24]. In these cases, histological evaluation does not appear adequate to differentiate talc pneumoconiosis from asbestosis. Moreover, talc can penetrate the lung through the lymphatic vessels and may lead to the formation of a peri-bronchiolar granuloma or fibrosis resembling other pneumoconioses induced by asbestos minerals. Raman spectroscopy thus proves an useful tool, making it possible to analyze thin sections made for medical diagnosis of the disease to accurately distinguish inhaled fibres from inorganic phases introduced during treatment. In this study, direct micro-Raman spectroscopy of the inorganic phases observed in histological pleural-lung sections was coupled with chemical analysis performed by SEM/EDS (Scanning Electron Microscopy with Energy Dispersive Spectroscopy).

2. Experimental

To determine the characteristics of the powder used for pleurodesis (Talc de Luzenac, STERILTALC® F4, NOVATECH), its mineral composition was analyzed by the X-ray powder method using an X'TRA Thermo ARL Diffractometer working in θ:θ geometry, Cu (Kα) radiation and equipped with a "Peltier" detector. The spectra were recorded at a scan rate of 0.2°/min in a 2θ range 2-70° to detect mineral phases present even in very small amounts. The data were processed using the WinXRD software, version 2.0-5.

Pleura and/or lung samples from six patients, affected by MM, were first embedded in a paraffin block, and then sliced with a microtome into 3 μm thick sections. The sections were mounted and fixed on slides and then placed in an oven at 60° C, the melting point of the paraffin. In a departure from routine procedure, the sections were not stained with Haematoxylin & Eosin, to avoid the risk that their Raman bands might overlap with those of the inorganic particles/fibres under analysis. The sections were first observed under an OM equipped with two polarizers to identify the inorganic phases by means of their optical properties under crossed nicols. The crystals optically detected were analysed under micro-Raman spectroscopy using a Jobin Yvon HR800 LabRam μ-spectrometer equipped with an Olympus BX41 microscope, a HeNe 20 mW laser working at 632.8 nm and a CCD (charge-coupled device) air-cooled detector. The instrument was carefully calibrated by checking position and intensity of the Si band at ± 520.6 cm−1 before every run. To increase the signal to noise ratio, 50 repeats of 10 second integration time spectra were carried out. The spectra registered were processed using the ORIGIN software, version 6.0. The Raman region of interest was 1200-200 cm−1, containing the vibrational lattice modes identified by Rinaudo et al. [25] and [26] and useful for distinguishing the different asbestos minerals. Raman bands with an asymmetric appearance were processed with the curve-fitting tool of the OPUS software, version 4.0. Band fitting was carried out using a Gaussian function introducing the minimum number of component bands in the process. Fitting was performed until reproducible results were obtained with the minimum residual error.

After being characterized by micro-Raman spectroscopy, each particle/fibre was studied under VP-SEM/EDS, Variable Pressure SEM/EDS, model E-SEM Quanta 200, FEI company, equipped with an EDS

microprobe, EDAX, for microanalysis. This instrument allows samples to be characterized without being coated first, so the inorganic phases can be identified directly in the biological matrix in which they are incorporated. The value of pressure used was 90 Pa, under 20 kV accelerating voltage; the spectra registered were processed using the GENESIS software, version 3.6. The inorganic particles/fibres were very small and thin, so to determine the contribution of the cellular composition to the chemical values obtained under EDS, analyses were always performed either on the inorganic particle/fibre (IN) or in areas external (OUT), close to it. The difference was then calculated between the average IN values and the average OUT values in order to obtain a qualitative analysis of the inorganic phase being examined.

After carbon coating of the thin section, quantitative chemical analysis of the phosphate particles was also carried out under a SEM Cambridge Stereoscan S360 equipped with an EDS, Oxford INCA Energy 200 coupled with a SATW PentaFET detector. The accelerating voltage was 15 kV. Quantitative data were calculated by means of the INCA Microanalysis Suite software package, version 4.08, using the reference standards of albite for Na, periclase for Mg, apatite for P and wollastonite for Ca.

3. Results

The X-ray spectrum of the powder used for pleurodesis is shown in Fig. 1. As expected, talc appears as the predominant phase; in fact, almost all of the peaks detected may be ascribed to the same mineral: phyllosilicate, with the chemical composition Mg6[Si8O20](OH)4[27]. Nevertheless, other peaks (CHL in Fig. 1), which were weak in intensity, on the spectrum and not ascribable to talc were also observed. These can be assigned to clinochlore, a mineral phase with the chemical composition [(Mg10Al2)(Si6Al2O20)(OH)16], in which substitutions of Fe for Mg may occur [27]. This mineral, too, is a phyllosilicate, but it belongs to the family of clay minerals. This last phase is therefore an impurity in the powder used for talc-pleurodesis.

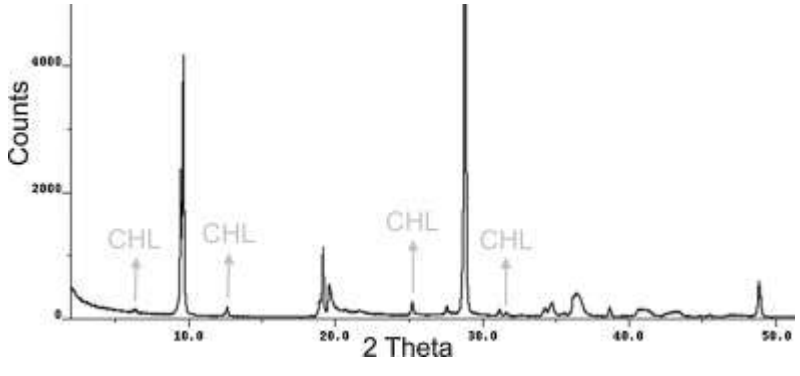

Fig. 1.

X-ray powder pattern of the powder used for pleurodesis. All the observed peaks, except for the peaks indicated as CHL, are ascribed to Talc; CHL peaks are ascribing to clinochlore, present as an impurity in the powder (Talc de Luzenac, STERILTALC® F4, NOVATECH).

When analysed under the OM, thin sections from the patients affected by MM and undergone pleurodesis show a parietal and visceral pleura characterized by a fibrosclerotic process, a residual area of mesothelioma and a band of granulomatous reaction with strong birefringent crystals, Fig. 2, onto which the laser of the spectroscope was focussed. Two types of spectra were registered:

a)

in the majority of cases and on the thinner crystals, as shown in Fig. 3a, the spectrum shown in Fig. 3b was obtained: the wavenumbers of the Raman bands and their relative intensities identify the phase as talc [16];

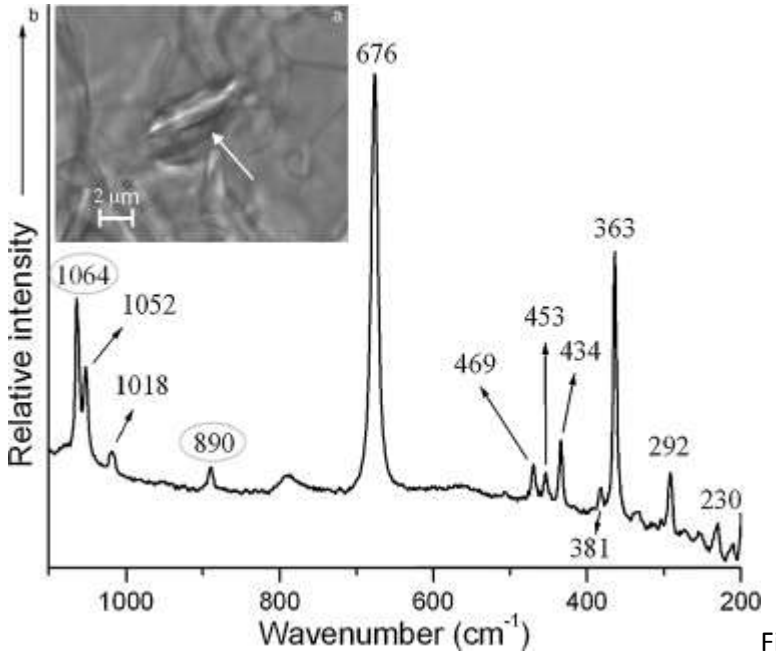

Fig. 3.

(a) An elongated crystal analysed by micro-Raman spectroscopy. (b) Raman spectrum registered on the crystal shown in Fig. 3a and obtained on a great number of the elongated crystals examined. The wavenumbers of the Raman bands and their relative intensity indicate talc. Circled bands are produced by the paraffin film covering the thin section.

b)

sometimes, on thicker crystals, Fig. 4a, the spectrum reported in Fig. 4b was registered; the wavenumbers of the Raman bands allow this phase to be ascribed to “clinochlore”.

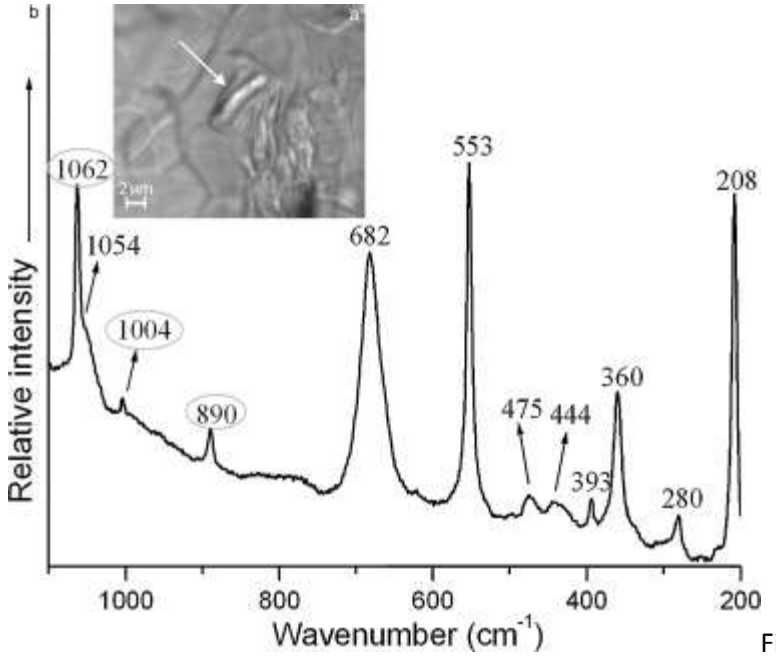

Fig. 4.

(a) More thick crystal on which the Raman spectrum indicating chlinoclore was registered. (b) Raman spectrum sometimes registered and corresponding to clinochlore. Circled bands are produced by the paraffin film covering the thin section.

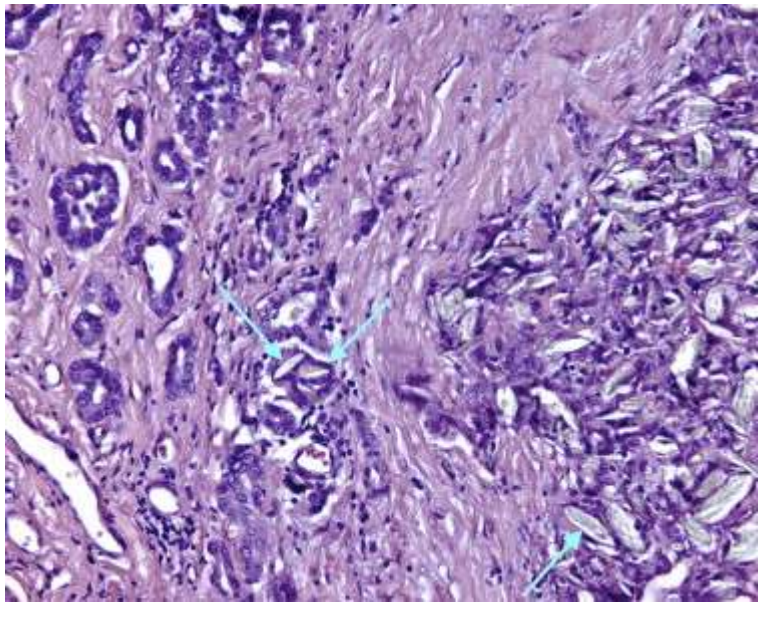

Fig. 2.

Optical photograph of pleural section: on the left, neoplastic mesothelial proliferation; on the right, a granulomatous reaction to the powder used for pleurodesis. In this case, the histological section has been treated with haematoxylin and eosin to better highlight the cellular medium around the inorganic phases.

It must be emphasized that, in Fig. 3b and 4b, all the bands characterizing the Raman spectra from the natural samples of talc [15] and of clinochlore can be seen [28] and [29]. We read this spectroscopic behaviour as an indication of a three-dimensional crystal structure of the injected mineral phases that is not strongly affected by interaction with the cellular medium. As for the chemical composition of the crystals studied under micro-Raman spectroscopy, as expected, VP-SEM/EDS analysis reveals Si and Mg as constituting ions for talc (Fig. 5a) and Si, Al, Mg and very small amounts of Fe for chlinoclore (Fig. 5b). The phase recognition obtained by Raman spectroscopy is therefore confirmed by VP-SEM/EDS analysis.

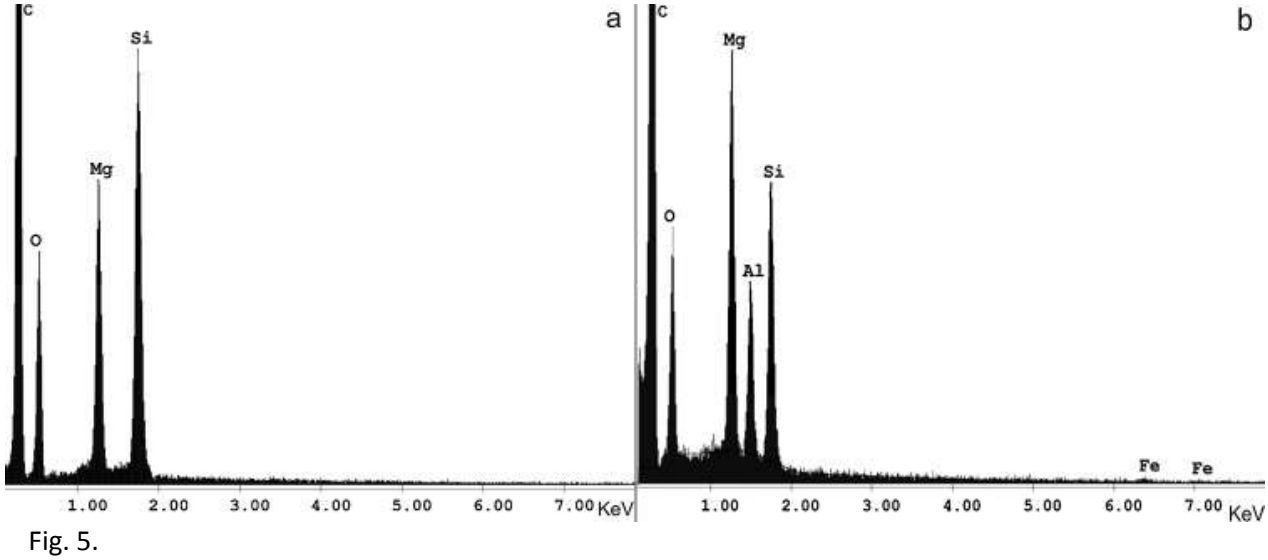

Fig. 5.

(a) Energy spectrum registered under VP-SEM/EDS on the same Fibre as that shown in Fig. 3a showing Mg, Si and O as constituting ions, as expected for talc. (b) Energy spectrum registered under VP-SEM/EDS on the fibre in Fig. 4a and showing Mg, Si, Al, very small amounts of Fe and O as constituting ions, as expected for clinochlore.

In addition to talc and chlinoclore crystals, many rounded formations measuring just a few microns in size were also observed in the pleural tissue (Fig. 6a and 6b). On the larger particles, which appear optically darker, the Raman spectrum reported in Fig. 7 was registered. The band wavenumbers allowed these particles to be ascribed to “hydroxyapatite” (HA), a phosphatic mineral with the chemical formula [Ca5(PO4)3(OH)] and typical of bone tissue. VP-SEM/EDS analysis performed on the same particles confirmed the presence of Ca, P, and O as the main constituting ions, as seen in Table 1. Many of the smaller rounded particles yielded the spectrum in Fig. 8a. This spectrum has only a few bands, the most

intense of which appears at 972 cm−1, 10 cm−1 away from the most intense band in the HA spectrum. Three large humps lie near 1080, 560 and 405 cm−1. The band at 972 cm−1 appears asymmetric, so a fitting of this band was carried out. Two components were identified, with the first, more intense one at 972 cm−1, and the other at 965 cm−1 (Fig. 8b). The bands in the Raman spectrum in Fig. 8a show wavenumbers detected on the Raman spectra from β-tricalcium phosphate (β-TCP), β-Ca3(PO4)2, a phase which crystallizes, depending on pH, Ca/P ratio and aging time, during the synthesis of the HA [34]. Nevertheless, data in the literature indicate that the spectra of β-TCP show two well-separated bands in the spectral region 980-950 cm−1: a more intense one near 970 cm−1 and another less intense near 946 cm−1. A shoulder at 961 cm−1 is also reported [30], [31], [32], [33], [34], [35] and [36]. In our case, the band at 972 cm−1 always appeared intense, with a marked shoulder at 965 cm−1, whereas the band at 946 cm−1 was never observed. For this reason, chemical quantitative microanalysis was carried out on the rounded crystallizations showing the Raman spectrum in Fig. 8a; the results from different particles are shown in Table 2. From the chemical data, Mg and Na appear replacing Ca in the crystal structure and a formula, calculated on the basis of 8 oxygens, (Ca2,71Mg0,25Na0,14)Σ3.1P1,99O8 may be proposed. Mg is reported to play a stabilizing role in the β-TCP structure by Dickens et al., 1974 [37], and Na has recently been reported by Quillard et al., 2011 [38] as replacing Ca in phosphates during the crystallization of Na and/or K substituted β-TCP. Moreover, considering that the Ca/P ratio expected for apatite is 1.67 and for β-TCMP ≤ 1.5 [31], on the basis of the SEM/EDS composition we may hypothesize crystallization of a phase close to β-TCMP [35]. However, in an experiment of mineralization in osteoblast cell cultures, and therefore in biological systems, Stewart et al. (2002) observed the crystallization of a phase showing on the Raman spectra only one large band at 975 cm−1; they assigned this phase to β-TCP [36].

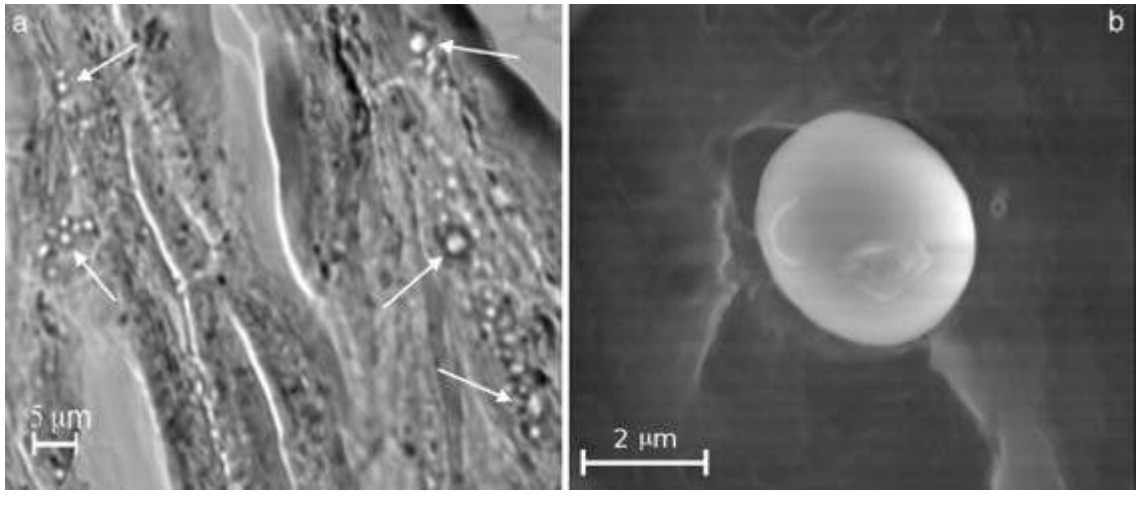

Fig. 6.

(a) Rounded particles observed by optical microscope in the pleura. (b) The same type of particles observed under Scanning Electron Microscopy (SEM), allowing determination of their size as a few microns.

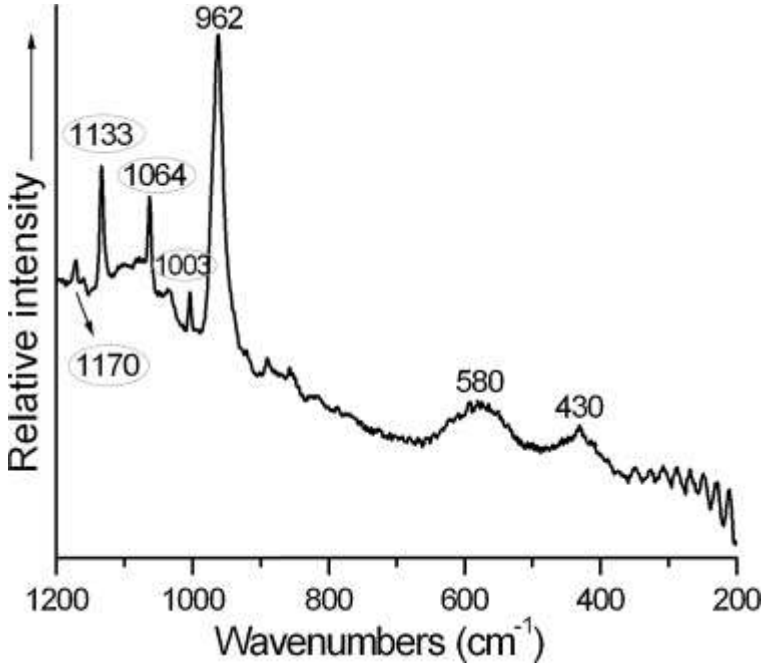

Fig. 7.

Raman spectrum registered on a larger particle, like that shown in Fig. 6b, indicating hydroxyapatite, a calcium phosphate mineral; the circled bands are produced by the paraffin covering the histological section.

Table 1.

Atomic %

Analyses IN	**C**	**O**	**Si**	**Mg**	**Ca**	**P**	**Na**	**S**
an01_in	89,84	6,01	0,61	0,17	1,66	1,32	0,40	0,00
an02_in	88,74	6,75	0,65	0,00	1,92	1,50	0,45	0,00
an03_in	89,50	5,70	0,74	0,16	1,99	1,51	0,40	0,00
mean_IN	*89,36*	*6,15*	*0,67*	*0,11*	*1,86*	*1,44*	*0,42*	*0,00*
Analyses OUT	C	O	Si	Mg	Ca	P	Na	S

Atomic %

Analyses IN	**C**	**O**	**Si**	**Mg**	**Ca**	**P**	**Na**	**S**
an01_out	94,23	3,56	1,54	0,10	0,14	0,00	0,39	0,05
an02_out	94,10	2,70	2,36	0,14	0,23	0,00	0,40	0,08
mean_OUT	*94,17*	*3,13*	*1,95*	*0,12*	*0,19*	*0,00*	*0,40*	*0,07*
MEAN'S DIFFERENCE	-4,81	3,02	-1,28	-0,01	1,67	1,44	0,02	-0,07

VP-SEM/EDS analyses performed on a rounded crystal corresponding to hydroxyapatite on the basis of the Raman spectrum in Fig. 7. The values are expressed in atomic percent. The first three analyses were carried out on the particle (IN); the other two analyses in the area external, but close to it (OUT). Mean values of the three IN analyses and of the two OUT analyses were calculated and the difference represents the ions composing the analyzed particle: O, Ca and P, as expected for hydroxyapatite.

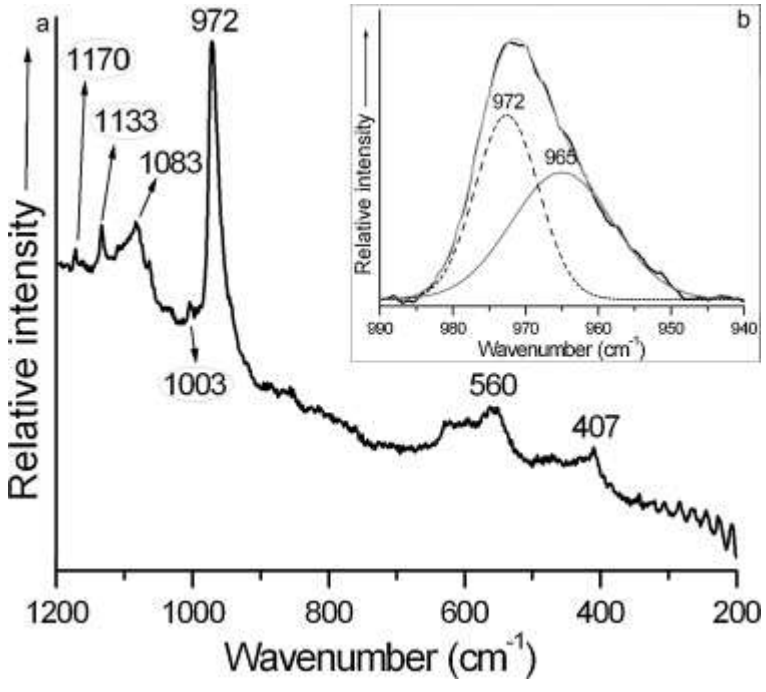

Fig. 8.

(a) Raman spectrum registered on smaller rounded particles, crystallization of a phase close to β-TCMP may be hypothesized. (b) Fitting of the most intense band at 972 cm−1 in the Raman spectrum reported in Fig. 8a.

ANALYSES	Ca	Mg	Na	P	Σ	O	(Ca + Mg + Na)/P
An #01	2,69	0,25	0,15	2,00	5,08	8	1,54
An #02	2,67	0,23	0,12	2,01	5,04	8	1,51
An #03	2,67	0,24	0,17	2,00	5,08	8	1,54
An #04	2,73	0,25	0,14	1,98	5,10	8	1,57
An #05	2,78	0,26	0,10	1,96	5,11	8	1,61
An #06	2,74	0,27	0,18	1,96	5,15	8	1,63
Mean Values	*2,71*	*0,25*	*0,14*	*1,99*	*5,09*	*8*	

Table 2.

Cations from quantitative SEM/EDS analyses performed on different rounded particles showing Raman spectrum in Fig. 8. The data were normalized to 8 O atoms.

Phosphates were not detected in the powder used for pleurodesis by X-ray diffraction (Fig. 1) or under VP-SEM/EDS when the technique was applied on the starting talc used for pleurodesis to rule out a concentration of phosphate phases so low as to be undetectable by X-ray diffraction (<1%). The results described make it reasonable to hypothesize the crystallisation of these phosphate phases in the pleura of patients affected by MM. On the other hand, pulmonary calcifications and ossifications caused by different diseases are described by Chan et al. (2002) [39]; in the cases studied, it seems that the precipitation of β-TCMP and of HA occurs in the pleura.

On the thin sections of lung tissue, near the talc-chlinoclore elongated crystals observed in the pleura, several “asbestos bodies”, like those represented in Fig. 9a and 9b, were identified in the lung. Micro-Raman spectroscopy was applied on these corpuscles in an attempt to identify the mineral phase inside the coating material. Considering the “asbestos body” in Fig. 9b, when the laser beam was directed on the area indicated by the arrow in the figure, appearing less covered by the ferruginous coating material, the Raman spectrum shown in Fig. 10 was recorded. The wavenumbers of the Raman bands correspond to those most intense in the Raman spectra of the natural fibres of crocidolite, a mineral phase regulated as “asbestos” [25] and [40]. The same was obtained on other “asbestos bodies” in the thin sections examined.

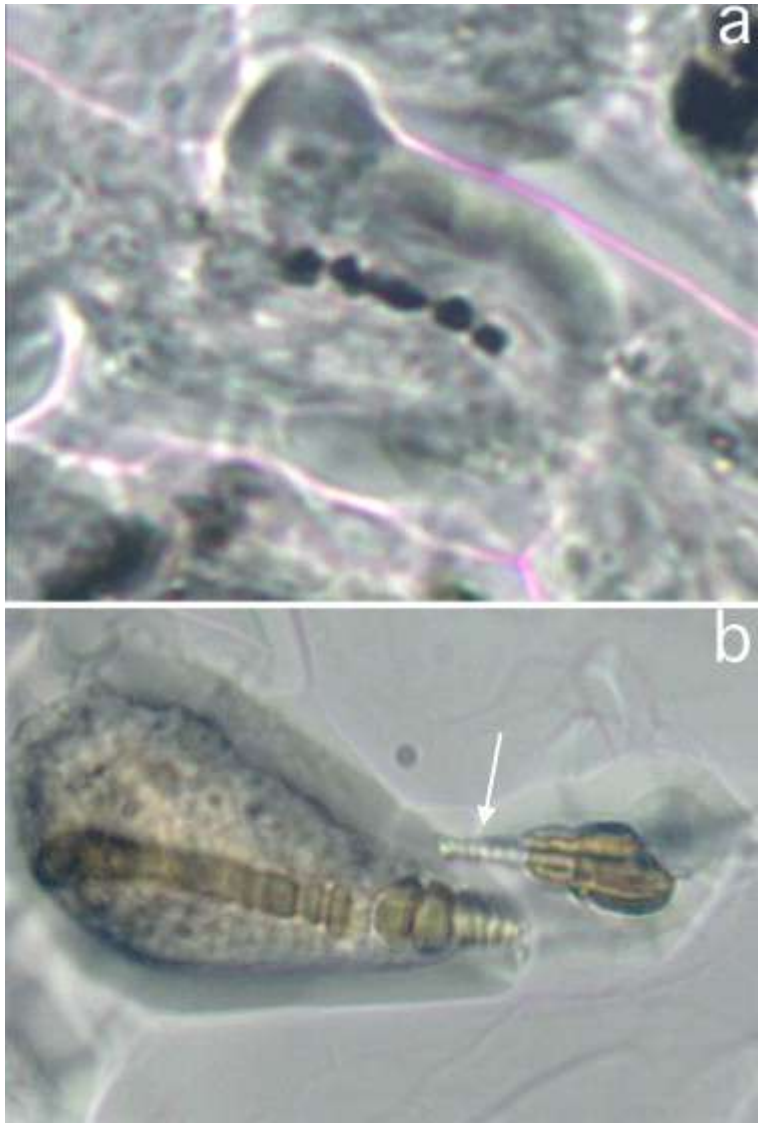

Fig. 9.

(a and b) “Asbestos bodies” observed in the lung tissue.

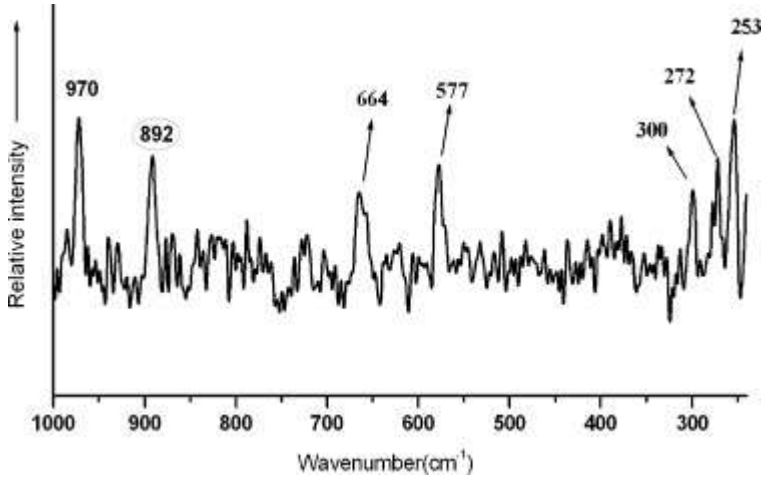

Fig. 10.

Raman spectrum registered addressing the laser beam on the part of the “asbestos body” arrowed in Fig. 9b and almost free of coating material. All the Raman bands, except for the band at 892 cm−1 which also belongs to the paraffin film, are typical of crocidolite, which therefore proves to be the mineral phase of the incorporated fibre.

4. Conclusions

Micro-Raman spectroscopy is an effective technique for identifying the inorganic phases contained in thin sections of pleura and lung prepared for medical diagnosis of MM, allowing mineral phases used for pleurodesis to be distinguished from the other phases detected. Pleurodesis produces the proliferation of fibroblastic cells arranged haphazardly in fascicles around birefringent crystals, whose Raman spectra correspond to talc or clinochlore. In the present study, fibrous talc and clinochlore appear uncoated, and their Raman spectra indicate that the three-dimensional network of the crystalline structure is poorly affected by the mineral-cell interaction. Precipitation of a phase appearing very near that of β-TCMP, whose crystallization is observed in bone tissue when the Ca/P ratio is ≤ 1.50, and of apatite, which grows when the Ca/P ratio is higher [31] and [34], is observed in the pleura of the patients. Observation by OM of the alveolated lung parenchyma revealed ferruginous bodies, whose Raman spectra indicated the presence of crocidolite, an asbestos mineral in the core. Micro-Raman spectroscopy does not require sample preparation and can be applied directly to histological sections prepared for medical diagnosis; moreover, it also makes it possible to determine the position of the inorganic phases in the tissue and the reaction of the cellular medium around them.

References

[1]

ME. Gunter, E., Belluso, A. Mottana, in: J.J. Rosso (Ed.), Reviews in Mineralogy and Geochemistry, Mineralogical Society of America Chantilly VA, 2007. Vol. 67, p. 453-516.

[2]

H. Fujiwara, T. Kamimori, K. Morinaga, Y. Takeda, N. Kohyama, Y. Miki, K. Inai, S. Yamamoto

Ind. Health, 43 (2005), pp. 346–350

[3]

M. Soffritti, F. Minardi, L. Bua, D. Degli Esposti

F. Belpoggi Eur. J. Oncol., 9 (2004), pp. 169–175

[4]

V. Cardile, M. Renis, C. Scifo, L. Lombardo, R. Gulino, B. Mancari, A.M. Panico

Int. J. Biochem. Cell Biol., 36 (2004), pp. 849–860

[5]

L. Lambertini, M. Padovani, D. Santini, M. Soffritti

Eur. J. Oncol., 8 (2003), pp. 215–219

[6]

A. Gianfagna, P. Ballirano, F. Bellatreccia, B. Bruni, L. Paoletti, R. Oberti

Mineral. Mag. 67, 6 (2003), pp. 1221–1229

[7]

P. Comba, A. Gianfagna, L. Paoletti

Arch. Environ. Health, 58 (2003), pp. 229–232

[8]

Z. Kartaloglu, A. Ilvan, R. Aydilek, K. Cerrahoglu, K. Tahaoglu, H. Baloglu, Z. Misirli

Yonsei Med. J, 44 (2003), pp. 169–173

[9]

A.B. Kane, V. Kumar, in: R.S. Cotran, V. Kumar and T.Collins,eds., W.B.Saunders (Ed.), Robbins pathologic basis of disease, Philadelphia, 1999. Chap. 10, p. 403.

[10]

F. Mollo, E. Pira, G. Piolatto, D. Bellis, P. Burlo, A. Andreozzi, S. Bontempi, E. Negri

Int. J. Cancer, 60 (1995), pp. 289–293

[11]

A.R. Brody

Environ. Health Perspectives, 100 (1993), pp. 21–30

[12]

G.D. Guthrie, B.T. Mossman, in: G.D. Guthrie, B.T. Mossman (Eds.), Reviews in Mineralogy, Mineralogical Society of America Washington, D.C. 1993. Vol. 28, p. 1-584.

[13]

G.D. Guthrie

Am. Mineral., 77 (1992), pp. 225–243

[14]

B. Mossman, W. Light, E. Wei

Annu. Rev. Pharmacol. Toxicol., 23 (1983), pp. 595–615

[15]

C. Rinaudo, M. Allegrina, E. Fornero, M. Musa, A. Croce, D. Bellis

J. Raman Spectrosc. 41, 1 (2010), pp. 27–32

[16]

C. Rinaudo, A. Croce, M. Musa, E. Fornero, M. Allegrina, P. Trivero, D. Bellis, D. Sferch, F. Toffalorio, G. Veronesi, G. Pelosi

Appl. Spectrosc. 64, 6 (2010), pp. 571–577

[17]

A.V. Gonzales, V. Bezwada, J.F. Beamis Jr., A.G. Villanueva

Chest 137, 6 (2010), pp. 1375–1381

[18]

J.P. Janssen

Monaldi Arch. Chest Dis., 61 (2004), pp. 35–38

[19]

J. Ferrer, M.A. Villarino, J.M. Tura, A. Traveria, R.W. Light

Chest, 119 (2001), pp. 1901–1905

[20]

H.G. Colt, J.F. Dumon

Chest, 106 (1994), pp. 1776–1780

[21]

R.L. Attanoos, A.R. Gibbs

Histopathology, 45 (2004), pp. 393–397

[22]

L. Mazzucchelli, H. Radelfinger, R. Kraft

Acta Cytol., 40 (1996), pp. 552–554

[23]

A.M. Churg, M.L. Warnock

Am. J. Pathol., 102 (1981) 447-445

[24]

E. Crouch, A. Churg

Am. J. Surg. Pathol., 8 (1984), pp. 109–116

[25]

C. Rinaudo, E. Belluso, D. Gastaldi

Mineral. Mag., 68 (2004), pp. 455–465

[26]

C. Rinaudo, D. Gastaldi, E. Belluso

Can. Mineral., 41 (2003), pp. 883–890

[27]

W.A. Deer, R.A., Howie, J. Zussman, in: Zanichelli (Ed.) Introduzione ai minerali che costituiscono le rocce 2nd ed., Bologna, 1994. p. 305, 313, 631.

[28]

A.K. Kleppe, A.P. Jephcoat, M.D. Welch

Am. Mineral., 88 (2003), pp. 567–573

[29]

A.C. Prieto, J. Dubessy, M. Cathelineau

Clay Clay Miner. 39, 5 (1991), pp. 531–539

[30]

P.N. De Aza, F. Guitián, C. Santos, S. de Aza, R. Cuscó, L. Artús

Chem. Mater., 9 (1997), pp. 916–922

[31]

B. Wopenka, J.D. Pasteris

Mat. Sci. Eng. C.-mater., 25 (2005), pp. 131–143

[32]

S. Koutsopoulos

J. Biomed. Mater. Res., 62 (2002), pp. 600–612

[33]

R. Cuscó, F. Guitián, S. de Aza, L. Artús

J. Eur. Ceram. Soc., 18 (1998), pp. 1301–1305

[34]

G. Penel, N. Leroy, P. Van Landuyt, B. Flautre, P. Hardouin, J. Lemaître, G. Leroy

Bone, 25 (1999), pp. 81S–84S

[35]

S. Kannan, A.F. Lemos, J.H.G. Rocha, J.M.F. Ferreira

J. Am. Ceram. Soc. 89, 9 (2006), pp. 2757–2761

[36]

S. Stewart, D.A. Shea, C.P. Tarnowski, M.D. Morris, D. Wang, R. Franceschi, D.L. Lin, E. Keller

J. Raman Spectrosc., 33 (2002), pp. 536–543

[37]

B. Dickens, L.W. Schroeder, W.E. Brown

J. Solid State Chem., 10 (1974), pp. 232–248

[38]

S. Quillard, M. Paris, F. Deniard, R. Gildenhaar, G. Berger, L. Obadia, J.M. Bouler

Acta Biomater., 7 (2011), pp. 1844–1852

[39]

E.D. Chan, D.V. Morales, C.H. Welsh, M.T. McDermott, M.I. Schwarz

Am. J. Respiratory and Critical Care Med, 165 (2002), pp. 1655–1669

[40]

Directive 2003/18/CE of the European Parliament and of the European Council of 27th March 2003.